RP4 Repressor Protein KorB Binds to the Major Groove of the Operator DNA: A Raman Study†

Lubomír Dostál,‡ Dheeraj Khare,§ Jiří Bok,|| Udo Heinemann,§,⊥ Erich Lanka,# and Heinz Welfle*,‡

AG Biopolymerspektroskopie and FG Kristallographie, Max-Delbrück-Centrum für Molekulare Medizin Berlin-Buch, Robert-Rössle-Strasse 10, D-13092 Berlin, Germany, Institute of Physics, Charles University, Ke Karlovu 3, CZ-12116 Prague 2, Czech Republic, Institut für Chemie/Kristallographie, Freie Universität Berlin, Takustrasse 6, D-14195 Berlin, Germany, and Max-Planck-Institut für Molekulare Genetik, Ihnestrasse 73, D-14195 Berlin, Germany

Received May 5, 2003; Revised Manuscript Received September 12, 2003

ABSTRACT: KorB is a member of the ParB family of bacterial partitioning proteins. The protein encoded by the conjugative plasmid RP4 is part of the global control circuit and regulates the expression of plasmid genes, the products of which are involved in replication, transfer, and stable inheritance. KorB is a homodimeric protein which binds to palindromic 13 bp DNA sequences [5′-TTTAGC($^{G}/_{C}$)GCTAAA-3′] present 12 times in the 60 kb plasmid. Each KorB subunit is composed of two domains; the C-domain is responsible for the dimerization of the protein, whereas the N-terminal domain recognizes and binds to the operator sequence (O_B). Here we describe results of a Raman spectroscopic study of the interaction of the N-domain with a double-stranded model oligonucleotide composed of the palindromic binding sequence and terminal 5′-A^{Br}U and AG-3′ bases. Comparison of the Raman spectra of the free KorB N-domain and O_B DNA with the spectrum of the complex reveals large differences. KorB-N binds in the major groove of the O_B DNA, and the interactions induce changes in the DNA backbone and in the secondary structure of the protein.

Plasmid RP4 is a member of *Escherichia coli* incompatibility group P (IncP-1α) (*1*, *2*). It is a self-transmissible, broad host range, resistance plasmid of ∼60 kb. IncP-1α plasmids are capable of conjugative DNA and protein transfer and maintain themselves in a wide variety of Gram-negative bacteria. Because of this promiscuity, they are of particular interest. Regulatory proteins KorB, KorC, KorA, and TrbA are major factors in control and coordination of replication, transfer, and partitioning functions (*3*−*7*) and contribute to a large extent to the survival strategies of IncP-1α plasmids. KorB plays a direct role in the partitioning of plasmid RP4 and functions as a transcriptional repressor of RP4 genes. It is a member of the ParB family of proteins that are encoded on plasmids and bacterial chromosomes and are involved in genome partitioning (*8*−*11*).

KorB, an acidic protein, is composed of 385 amino acids (39 011 Da) and exists in purified form as a dimer in solution (*12*). O_B,[1] the operator sequence [5′-TTTAGC($^{G}/_{C}$)GCTAAA-3′] of KorB, occurs 12 times in the RP4 genome and 11 times in the related IncPβ plasmid R751. The 12 O_B sites were classified according to their positions relative to RP4 promoters in three classes. Class I sites are located 39/40 bp upstream of a transcription start site, and class II sites map further upstream or downstream of promoters within 80−190 bp of a transcription start site. KorB represses promoters carrying these O_B sites (*4*, *5*, *13*−*15*). Class III O_B sites are more than 1 kb away from any known promoter, and whether KorB has effects on these sites has not been elucidated. KorB acts cooperatively with KorA in transcriptional repression of the *kilA*, *trfA*, and *korAB* operons. KorB is also involved in the negative control of *kilB* operons. According to their affinity for KorB, the 12 O_B sites are divided into three groups. Protein IncC1, a ParA analogue, enhanced binding of KorB to 11 of the 12 O_B sites (except O_B3). It was suggested that IncC1 influences the multimeric state of KorB and thus its binding to O_B DNA and flanking sequences.

The KorB monomer is composed of two domains, KorB-N and KorB-C. Clones were constructed expressing KorB-N and KorB-C separately, and the three-dimensional structure of KorB-C, consisting of 62 amino acids, was recently elucidated (*2*). KorB-C is mainly responsible for the dimerization of the protein, whereas KorB-N represents its DNA recognition and binding domain.

In this study, we analyze by Raman spectroscopy the binding of KorB-N to the 17 bp DNA segment (5′-A^{Br}-UTTTAGCGGCTAAAAG-3′/5′-C^{Br}UTTTAGCCGCTAA-AA^{Br}U-3′) modeling an O_B binding site of KorB. The 17 bp DNA contains two palindromic binding sites composed of

† This work was supported by the Deutsche Forschungsgemeinschaft (Graduiertenkolleg GK 80/1 to H.W. and continued support to U.H.) and the Fonds der Chemischen Industrie (U.H.).

* To whom correspondence should be addressed. Email: welfle@mdc-berlin.de. Fax/Tel.: +49−30−9406 2840. Mailing address: Dr. Heinz Welfle, Max-Delbrück-Centrum für Molekulare Medizin, Postfach 740238, D-13092 Berlin, Germany.

‡ AG Biopolymerspektroskopie, Max-Delbrück-Centrum für Molekulare Medizin Berlin-Buch.

§ FG Kristallographie, Max-Delbrück-Centrum für Molekulare Medizin Berlin-Buch.

|| Charles University.

⊥ Freie Universität Berlin.

Max-Planck-Institut für Molekulare Genetik.

[1] Abbreviations: O_B, KorB operator DNA sequence; ^{Br}U, bromodeoxyuridine; KorB-N, N-terminal domain of the KorB protein.

10.1021/bi034723h CCC: $25.00
Published on Web 11/19/2003

six base pairs, top strand sequences 5′-TTTAGC and 5′-GCTAAA, separated by a central GC base pair. Three 5′-Br-substituted uridine residues were inserted instead of thymines at the flanking terminal base pairs to facilitate the ongoing crystallographic analysis. The 17 bp DNA binds two KorB-N molecules. KorB-N is a recombinant protein composed of 178 amino acids comprising residues R117−K294 of the RP4 KorB sequence. A Raman difference spectrum was obtained by subtraction of the spectra of isolated KorB-N and 17 bp DNA from the spectrum of the KorB-N−DNA complex, revealing large spectral changes induced by complex formation.

MATERIALS AND METHODS

Chemicals. Isopropyl β-D-thiogalactopyranoside (IPTG) and ampicillin were obtained from Roth (Karlsruhe, Germany). All other chemicals were purchased from Merck (Darmstadt, Germany). Superdex 75, HiTrap Heparin, and Mono Q columns were from Amersham-Pharmacia (Freiburg, Germany).

Preparation of KorB-N, DNA, and the KorB-N−DNA Complex for Raman Measurements. A gene encoding KorB-N was overexpressed in *E. coli*, after induction with IPTG, and its product was purified in a manner similar to the preparation of wild-type KorB described elsewhere (*3*). For spectroscopic measurements, the samples were finally purified by gel filtration through a Superdex 75 column, equilibrated with 20 mM Tris-HCl (pH 7.6) and 50 mM NaCl. The protein samples were further concentrated in 5K MWCO Ultrafree Millipore tubes. Protein concentrations were determined from the absorbance at 280 nm using an extinction coefficient of 13 940 M^{-1} cm^{-1} (calculated using the Expasy server).

Oligonucleotides were purchased from Biotez (Berlin, Germany). Concentrations of DNA were determined spectrophotometrically using an extinction coefficient ϵ_{260} of 271 222 M^{-1} cm^{-1}. Equimolar amounts of each strand were mixed, heated to 95 °C, annealed by slow cooling, and purified by gel filtration using a Superdex 75 column equilibrated in 20 mM Tris-HCl buffer (pH 7.6) and 50 mM NaCl. Peak fractions were concentrated in 5K MWCO Ultrafree Millipore tubes.

The KorB-N−DNA complex was prepared by mixing KorB-N and 17 bp O_B DNA in a 2:1 molar ratio and subsequent gel filtration. The column and the buffer that were used were the same as in the final purification steps described above for the individual components. The samples were concentrated in a Millipore Ultrafree centrifugal filter device. The concentration of the complex was determined by measuring the absorbance at 260 nm and using the DNA extinction coefficient.

Raman Spectroscopy. Samples of approximately 15 μL were sealed in homemade cuvettes consisting of cylindrical quartz bodies with quartz bottom windows and Teflon stoppers. The concentrations were 15.4 mg/mL for DNA, 22 and 34.2 mg/mL for KorB-N, and 62 and 59 mg/mL for the KorB-N−DNA complex. Raman spectra were excited with the 488 nm line of a Coherent Innova 90 argon laser using 100 mW of radiant power in the sample space. Spectra were collected at 22 °C on the model T64000 Raman spectrometer (Jobin Yvon) in a single mono configuration equipped with a liquid nitrogen-cooled charge-coupled-device (CCD) detector. Fifteen spectra, each measured for 120 s, were accumulated and averaged to produce the spectra shown in Figures 1−3. To exclude all possible drifts of the wavenumber scale during the measurements, a calibration spectrum was collected after each 120 s accumulation step of sample spectra. The description of the calibration procedure is given below.

Raman data analyses, including all spectra manipulations, were performed with the software packages LabSpec (Jobin Yvon) and GRAMS (Thermo Galactic). Solution spectra were corrected by subtraction of the buffer spectrum and fluorescence background that was approximated by a polynomial curve. For calculation of the difference spectrum, intensity differences between the spectra of isolated components and the KorB-N−DNA complex must be minimized. To achieve this, at first the spectra of isolated components were normalized with respect to the Raman band near 1092 cm^{-1}. The 1092 cm^{-1} band is assigned to the P−O stretching vibration of the phosphodioxy group (PO_2^-) and was shown to be invariant upon binding of the repressor protein to operator DNA (*16*). Then, the normalized but not otherwise corrected experimental spectra of 17 bp DNA and KorB-N were subtracted from the spectrum of the KorB-N−DNA complex. In the next steps, the buffer spectrum and, finally, fluorescence background were removed.

Difference bands are considered significant when the following criteria are fulfilled. (i) Their intensity is at least 2 times higher than the signal-to-noise ratio, and (ii) the difference bands reflect intensity changes of at least 5% of their parent bands.

Calibration. For the comparison of Raman spectra and for the calculation of difference spectra, the accuracy of the peak positions is crucial. Several factors can influence the wavenumber accuracy; moving of the grating especially could be a source of minor shifts which cannot be avoided by standard calibration procedures. To guarantee a high accuracy of the calibration, it is necessary to collect a calibration spectrum with sharp lines of exactly known peak positions immediately after each sample measurement. The neon glow lamp as an emission source provides an ideal calibration spectrum. It is composed of many lines that are suitable for calibration in the 489−640 nm region. Argon or mercury might be present as contaminations in some lamp fillings and provide additional lines which are useful for calibration purposes.

The calibration of the sample spectrum is performed in four steps by our program BERKAL1: (i) determination of the accurate peak positions in the neon glow lamp calibration spectrum, (ii) assignment of these peaks to the tabulated lines of neon (argon and mercury), (iii) least-squares fit of wavenumber versus pixel position for the identified lines, and (iv) conversion of the sample spectrum pixel scale to the wavenumber scale.

During the first step, the program finds the positions of all peaks in the neon glow lamp calibration spectrum which are significantly higher than the noise (typically ∼50 peaks). Then, these peak positions are refined up to subpixel resolution by Gaussian curve fitting. In the second step, the program assigns some peaks of the calibration spectrum to the tabulated lines (the program contains a table of suitable selected spectral lines with their wavelengths and positions on the pixel scale of a virtual CCD detector with 10 300

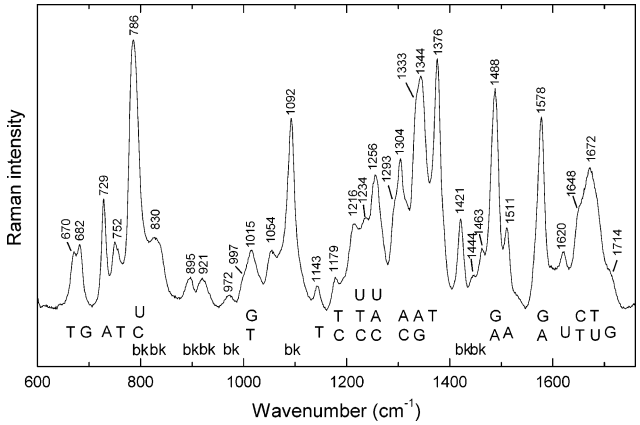

FIGURE 1: Raman spectrum of a 17 bp oligonucleotide designed as an operator DNA model (5′-A^{Br}UTTTAGCGGCTAAAAG-3′/5′-C^{Br}UTTTAGCCGCTAAAA^{Br}U-3′) in the region 600−1750 cm^{-1}. The sample buffer is 20 mM Tris (pH 7.6) and 50 mM NaCl; data were collected at 22 °C. Peak positions of prominent Raman bands are labeled. Wavenumbers are accurate to within ±0.5 cm^{-1}. Abbreviations are as follows: G, guanine; T, thymine; C, cytosine; A, adenine; U, uracil; bk, deoxyribose backbone.

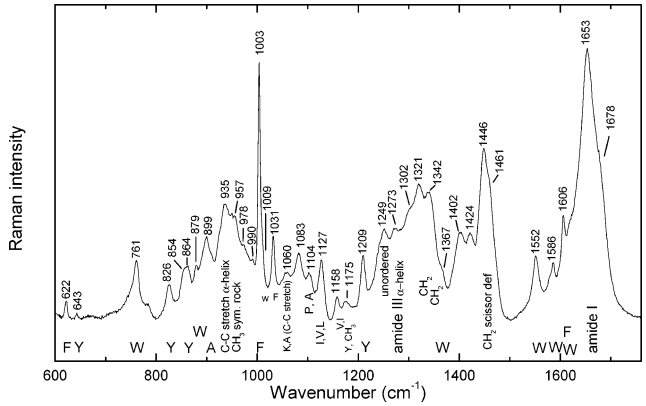

FIGURE 2: Raman spectrum of KorB-N in the region of 600−1750 cm^{-1}. The sample buffer is 20 mM Tris (pH 7.6) and 50 mM NaCl; data were collected at 22 °C. Peak positions of prominent Raman bands are labeled with the respective wavenumbers. Wavenumbers are accurate to within ±0.5 cm^{-1}. One-letter code is used for amino acids. Abbreviations are as follows: CH_2, methylene; CH_3, methyl; C−C, carbon−carbon bond.

pixels). The pixel peak positions only and not the peak intensities are used for the assignments. After step ii, the program has information about the pixel positions and corresponding wavenumbers of approximately 10 peaks (where the wavenumber is the Raman shift between the wavelength of the neon line and the laser excitation line). The pixel−wavenumber data pairs are fitted by a cubic polynomial that is used for the conversion of the sample spectrum from the pixel scale into the precise wavenumber scale.

RESULTS AND DISCUSSION

Raman Spectrum of the Unbound 17 bp O_B DNA. The Raman spectrum of the 17 bp O_B DNA in the 600−1760 cm^{-1} wavenumber region is shown in Figure 1. Wavenumber positions of the major peaks as given in the figure are in accordance with those given previously in the literature (refs *17*−*20* and references therein).

The backbone conformation markers at 830 and 1092 cm^{-1} are diagnostic of B-DNA (*18*), and the nucleoside conformation markers at 670 (dT), 682 (dG), 729 (dA), 752 (dT), and 1256 cm^{-1} (dC) identify C2′-*endo*/*anti* conformers. The spectrum is the signature of the O_B DNA model and provides the basis for the interpretation of the difference spectrum.

Raman Spectrum of KorB-N. Figure 2 shows the Raman spectrum of KorB-N with wavenumber positions of the major peaks, and peak assignments of amide I (1640−1680 cm^{-1}) and amide III bands (1230−1300 cm^{-1}), bands of aromatic and nonaromatic amino acids, and the α-helical skeletal mode (∼935 cm^{-1}). Assignments were made according to the literature (refs *21* and *22* and references therein).

Secondary Structure of KorB-N. α-Helices are the principal type of secondary structure of KorB-N as indicated by positions of main chain vibrations of the amide I and amide III bands. The prominent amide I peak centered at 1653 cm^{-1}, the intensity at 1273−1302 cm^{-1} in the amide III region, and the high intensity in the C−C stretch region around 940 cm^{-1} indicate a high content of α-helices. The 1237 cm^{-1} shoulder of the amide III peak at 1249 cm^{-1} points to a minor contribution of β-structures to the spectrum. The intense amide III band at 1249 cm^{-1} and the shoulder of the amide I band near 1678 cm^{-1} indicate the presence of irregular and turn structures.

Environment of Tyrosine Side Chains. A tyrosine doublet at ∼850 and ∼830 cm^{-1} is caused by Fermi resonance of the normal mode ν_1 (ring breathing fundamental) and the second harmonic $2\nu_{16a}$ (ring deformation overtone) of the para-substituted phenolic side chain (*23*). The I_{850}/I_{830} intensity ratio is sensitive to hydrogen bonding of phenolic OH groups and, therefore, an indicator of the tyrosine environment. In the spectrum of KorB-N, a sharp peak appears at 826 cm^{-1} and a rather broad peak around 858 cm^{-1} at the position of the tyrosine doublet. The I_{858}/I_{826} intensity ratio of 1.5 is in the range expected for tyrosines acting as both the donor and acceptor of moderately strong hydrogen bonds as is the case when they are exposed to solvent H_2O molecules (*23*). The sharp 826 cm^{-1} peak obviously belongs to the Fermi doublet of Y2 and Y21, the two tyrosines present in the chain of KorB-N. The broad 858 cm^{-1} peak can be decomposed into two bands at 854 and 864 cm^{-1}. The 864 cm^{-1} band possibly arises from an aromatic side chain that is yet to be assigned.

Tryptophan. Two Trp residues, W7 and W114, contribute to the spectrum of KorB-N (Figure 2). Indole ring vibrations of W7 and W114 cause the peak at 879 cm^{-1} (called the W17 mode) and a 1367 cm^{-1} shoulder of the 1342 cm^{-1} peak. The 879 cm^{-1} band position in the KorB-N spectrum is indicative of exposed Trp residues with hydrogen bonds of medium strength between the exocyclic Trp 1NH donors and water molecules. The Trp vibrations are sensitive to the indole ring environment; buried residues form sharp intense peaks, whereas the intensity is low for exposed residues. For the W17 mode, a frequency range between 883 and 871 cm^{-1} was observed; without H-bonding at the N1 site, this band is located at 883 cm^{-1}, and at 871 cm^{-1} with strong H-bonding (*24*).

The frequency of the Trp band near 1550 cm^{-1} (called the W3 mode) assumes values between 1542 and 1557 cm^{-1} depending on the absolute value of the $C_\alpha C_\beta C_3 C_2$ torsion angle $|\chi^{2,1}|$ which varies between 60° and 120° (*25*). The 1552 cm^{-1} position of the Trp band indicates an average $|\chi^{2,1}|$ value of ∼90° for the two Trp residues of KorB-N.

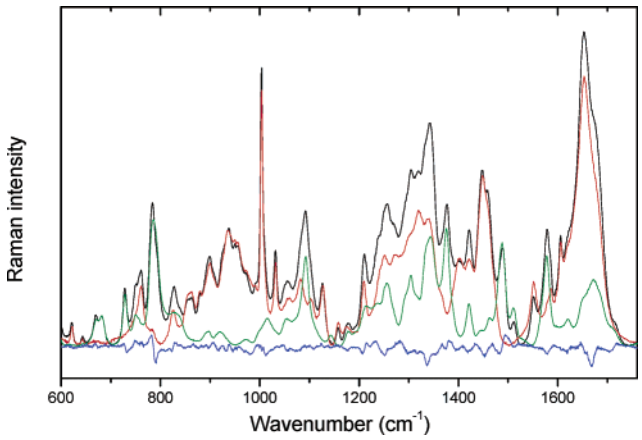

FIGURE 3: Raman spectrum of KorB-N in complex with 17 bp operator DNA (KorB-N−DNA) in the region 600−1750 cm^{-1} (black trace). The red trace shows the Raman spectrum of the isolated protein from Figure 2. The green trace shows the Raman spectrum of DNA from Figure 1. The blue bottom trace shows the computed difference spectrum obtained by subtraction of the isolated component spectra from the experimental spectrum of the complex. The spectra are normalized to represent the same amounts of protein and DNA in the complex and in the free form.

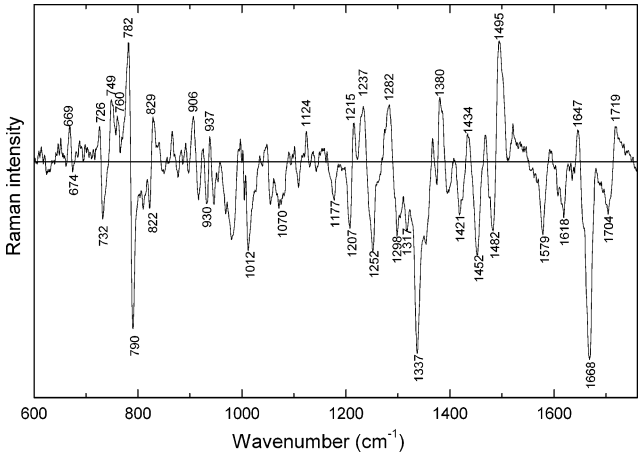

FIGURE 4: Enlarged Raman difference spectrum (blue bottom trace from Figure 3). The spectrum was smoothed using the 11-point Savitsky−Golay algorithm.

Raman Analysis of the KorB-N−DNA Complex. The Raman spectrum of the KorB-N−DNA complex is shown at the top of Figure 3 (black trace). The green trace represents the DNA spectrum from Figure 1, and the red trace is the KorB-N spectrum from Figure 2. The blue trace is the difference spectrum obtained by subtraction of the component spectra (green and red traces) from the spectrum of the complex (black trace). A positive difference peak indicates an increased Raman intensity at the respective wavenumber region in the spectrum of the complex compared to the sum of component spectra, and a negative trough is caused by a lower intensity in the spectrum of the complex.

The amplified and, for clarity, smoothed difference spectrum from Figure 3 (blue trace) is shown in Figure 4 and used for the further analysis. The features of the difference spectrum provide information about conformational changes, structural rearrangements, and interactions between DNA and protein. A reliable and detailed interpretation of the difference bands is easier in spectral regions with separate vibrations of DNA and protein and difficult where bands of both components overlap.

Backbone and Deoxynucleoside Conformation of the DNA. The 600−900 cm^{-1} region contains Raman markers with a deoxynucleoside conformation and DNA backbone geometry (*18*). The peaks at 670 and 682 cm^{-1} in the spectrum of the O_B DNA (Figure 1) are thymine and guanosine nucleoside conformation markers, respectively, for B-DNA and sensitive to an altered deoxynucleoside conformation. In the difference spectrum, there is a peak at 669 cm^{-1} and a trough at 674 cm^{-1}. This feature possibly reflects a minor downward shift of the 670 cm^{-1} thymine band. A difference feature with a peak at 726 cm^{-1} and a trough at 732 cm^{-1} is observed, indicating a downward shift of the 729 cm^{-1} adenosine marker band. The peak at 749 cm^{-1} is probably caused by a downshift or intensity change of the 752 cm^{-1} band of thymidine. Altogether, these difference features are evidence of an altered deoxynucleoside conformation of thymidine and adenosine in the complex.

A 782 cm^{-1} peak in the Raman spectra of DNA is assigned to cytosine, and a 794 cm^{-1} peak is assigned to a stretching vibration of backbone phosphodiester groups and diagnostic of B-DNA backbone geometry, specifically of torsion angles α and ζ in the *gauche*$^-$ range (*26*). The 782 cm^{-1} cytosine and 794 cm^{-1} backbone bands overlap in the O_B DNA spectrum to a large 786 cm^{-1} peak. In the difference spectrum, a prominent derivative feature (∼20% relative intensity change) with a peak at 782 cm^{-1} and a trough at 790 cm^{-1} is located in this region. The difference feature may be caused by changes in one or both bands signalizing cytosine interactions and/or changes in the backbone conformation.

In the difference spectrum, a clear derivative feature is present with a trough at 822 cm^{-1} and a peak at 829 cm^{-1}. In this region, the 830 cm^{-1} B-DNA backbone band and the 826 cm^{-1} peak of tyrosine overlap; therefore, this difference feature could be caused by DNA and/or protein contributions. The derivative feature suggests an intensity shift centered near 826 cm^{-1} and therefore points to a minor frequency change of the Tyr band. Another possible explanation is a shift to higher wavenumbers of the GC conformation marker band because of its location at 828 ± 2 cm^{-1} (*16*, *18*).

Deoxyribose Ring and Protein CH_2 and CH_3 Vibrations. Furanose vibrations were identified in Raman spectra of DNA at 1419 and 1455 cm^{-1} and assigned to backbone vibrations (*26*). In the spectrum of the 17 bp O_B DNA, the peak positions of these bands are at 1421 and 1463 cm^{-1}, and a further minor peak is located at 1444 cm^{-1}. Protein bands are also located in this spectral region. A COO^- symmetric stretch vibration causes the 1402 cm^{-1} peak; a band at 1424 cm^{-1} reflects CH_2 and CH_3 deformations, and at 1446 cm^{-1}, CH_2 scissoring modes are found. Therefore, the difference features observed between 1418 and 1452 cm^{-1} may be assigned to backbone vibrations of the DNA and/or changes in the protein. These backbone vibrations are mainly caused by 2′-CH_2 scissoring vibrations of the furanose residues which, coming in contact with protein side chains, are influenced and give rise to the observed difference feature. Also, CH_2 and CH_3 scissoring modes of the protein side chains may contribute to the difference spectrum. The contributions of the DNA may potentially be caused by alterations of the DNA helix geometry as induced by bending and/or unwinding as described for a SRY HMG box−DNA complex (*26*).

Major Groove Binding of KorB-N. Protein−DNA complexes studied by Raman spectroscopy provide examples of major groove binding, minor groove binding, and interaction with single-stranded DNA (*16*, *19*, *20*, *26*−*29*). Recently, Raman markers of different protein−DNA recognition motifs were proposed (*19*). Comparison of features of the KorB-N−DNA difference spectrum with proposed Raman markers will be discussed below.

Raman bands in the interval of 1300−1750 cm^{-1} are sensitive to specific interactions of major groove-binding proteins with DNA bases (*19*, *20*, *28*, *29*). Several features of the KorB-N−DNA difference spectrum indicate major groove binding.

The prototype Raman marker of protein−DNA interaction in the major groove is considered the guanine band near 1490 cm^{-1}. At this spectral position, Raman intensities of G and A overlap, with a significantly larger contribution from G. Therefore, in the spectra of DNA, the intensity of this band strongly depends on the base composition of the DNA. For DNA composed of only A and T base pairs, the band is weak and located at 1482 cm^{-1} (*30*). This band shifts to near 1470 cm^{-1} upon donation of a hydrogen bond to the N7 guanine ring acceptor (*16*, *20*, *28*), resulting in a characteristic derivative band profile with a difference peak at ∼1470 cm^{-1} and a trough at ∼1490 cm^{-1}. Such a derivative band profile is clearly missing in the difference spectrum of the KorB-N−DNA complex. Instead, in this spectral region, a large trough at 1482 cm^{-1} and a large peak at 1495 cm^{-1} are observed. Therefore, according to this criterion, we have no evidence for direct participation of guanine N7 in KorB-N binding. Also, the observed difference feature is not caused by purine unstacking which would yield a difference peak at 1494 cm^{-1} (*19*, *26*) but not the observed difference feature. Further possible explanations include minor groove binding of KorB-N and changes of the adenine vibration near 1485 cm^{-1}. Because major groove binding is indicated by established Raman markers (see below), minor groove binding is not likely. However, contacts of KorB residues with adenine bases in the major groove or a reduced level of fraying (see below) might be responsible for the observed difference feature provided that very pronounced perturbation of the weak adenine band is induced by those effects.

Major groove binding of proteins may cause a reduction in Raman intensity at 1717 cm^{-1} that can be attributed to guanine O6 interactions (*16*, *28*) and lead to a trough in the difference spectrum. For the free DNA, a corresponding band is identified at 1714 cm^{-1}, and in the difference spectrum, a derivative feature with a trough at 1704 cm^{-1} and a peak at 1719 cm^{-1} is observed. The difference feature indicates a surprisingly large change in the relative intensity and position of the G O6 band and provides an argument for major groove binding of KorB-N.

The adenine and guanine Raman marker bands at 1344 and 1578 cm^{-1} exhibit large effects upon protein binding (*26*, *31*) and probably cause the large difference troughs at 1337 and 1579 cm^{-1}. In the case of significant purine unstacking, an intensity increase for the 1344 and 1578 cm^{-1} bands and corresponding difference peaks in these spectral regions would be visible. However, difference peaks at ∼1340 and ∼1585 cm^{-1} are missing, and therefore, no significant purine unstacking is induced by KorB-N binding.

From experiments in which temperature effects on the Raman spectrum of poly(dA-dT)·(dA-dT) were analyzed, Raman markers were identified for premelting and melting transitions of AT-rich DNA sequences. Hydrogen bonding interactions between the bases and the geometry of the phosphodiester backbone are perturbed throughout the premelting (*32*). The most significant perturbation during premelting was observed near 1340 cm^{-1} in the band of adenine, which shifts from 1345 to 1330 cm^{-1} (1345 → 1330). Other significant temperature-dependent changes in adenine bands emerged near 1578 (1579 → 1571), 1511 (1516 → 1502), and 1485 cm^{-1} where a large increase in intensity was observed. During complex formation, an opposite effect could be expected, provided that binding of the protein is connected with increased stability of terminal A·^{Br}U base pairs which are fraying to some extent in the free DNA. Increased stability of the base pairs should cause a frequency shift of the 1330 and 1571 cm^{-1} adenine bands to 1344 and 1578 cm^{-1}, respectively, and a significant hypochromic effect. This explains the observed troughs near 1337 and 1578 cm^{-1}.

This interpretation is encouraged by the appearance of the trough at 1618 cm^{-1} assigned to bromodeoxyuridine. Bromodeoxyuridine is located at the ends of both strands of the oligonuclotide and base-paired with adenine. A reduced level of fraying of those A·^{Br}U base pairs should have a hypochromic effect on the 1620 cm^{-1} uridine band, and the reduced Raman intensity should cause a trough at this position as observed in the difference spectrum.

In DNA spectra, a peak at 1378 cm^{-1} is assigned to the thymine exocyclic $C5H_3$ group. Increased hydrophobicity in the surrounding thymine $C5H_3$ groups increases the intensity of the 1378 cm^{-1} band, as observed in the wild-type λ repressor−operator DNA complex (*16*), where the thymine $C5H_3$ groups are shielded by hydrophobic side chains of the repressor. Similarly, the difference spectrum of the KorB-N−DNA complex shows a large difference peak at 1380 cm^{-1} indicating shielding of thymine $C5H_3$ groups from the water environment. A small wavenumber shift from 1376 to 1380 cm^{-1} might be caused by an additional, still unidentified effect, e.g., interaction with protein groups. Thus, the 1380 cm^{-1} difference peak is consistent with KorB-N binding in the major groove. The interaction with thymine is further supported by a very large and sharp trough at 1668 cm^{-1} at the position of the thymine band at 1672 cm^{-1}.

The trough at 1012 cm^{-1} is located near the positions of the guanine/thymine band at 1015 cm^{-1} and of the 1009 cm^{-1} Trp shoulder of the sharp Phe band at 1003 cm^{-1}. A similar trough was observed for the omega−operator DNA complex involving a protein without Trp (*31*). Therefore, this difference peak may indicate interaction of guanine and/or thymine with KorB-N and can be considered a further hint of interactions of those bases in the major groove.

Changes in Side Chains of Nonaromatic Amino Acids of KorB. The difference spectrum of the KorB-N−DNA complex reveals perturbations in Raman bands of nonaromatic amino acids (C−C and/or C−N stretch, CH_2 and CH_3 vibrations) (*21*). Relevant features are a difference peak at 760 cm^{-1} (possible contributions of Trp and CH_2 rock of several amino acid side chains), difference features around 930 cm^{-1} (CH_3 symmetric rock), a broad difference trough at 1070 cm^{-1} (C−O stretch of serine, threonine, glutamic

acid, and aspartic acid, C−C stretch of alanine and lysine, and C−N stretch of proline, with possible problems related to buffer subtraction and potential overlapping of the PO_2^- vibration), a peak at 1124 cm^{-1} (C−C stretch of valine, leucine, and isoleucine), a trough at 1177 cm^{-1} (CH_3 symmetric rock, contribution of Tyr), and the troughs at 1337 cm^{-1} (lysine CH_2 twist/rock, alanine CH_2 bend, and a large contribution from DNA as discussed above) and 1452 cm^{-1} (C−C stretch and contribution from the 2′-CH_2 scissoring vibration of the DNA backbone). The large trough at 1452 cm^{-1} surrounded by small peaks on both sides shows widening and a slight shift of the 1446 cm^{-1} parent band assigned to CH_2 and CH_3 deformation vibrations. These perturbations show changes in the conformation of nonaromatic amino acid side chains. This may indicate structural rearrangements of KorB upon complex formation as well as interaction with O_B DNA.

Secondary Structure Changes of KorB-N. The difference spectrum of the KorB-N−DNA complex reveals significant but not very large spectral changes in the region between 1200 and 1340 cm^{-1} where the intensive bands of KorB-N (amide III, CH_2 twist/wag) overlap with the wide, intense 1256 cm^{-1} band of cytosine and thymine of the 17 bp O_B DNA. Thus, vibrations of protein, DNA, or both components of the complex can cause the observed features of the difference spectrum. The situation is similar in the 1640−1690 cm^{-1} region, where the intensive amide I protein bands overlap with guanine and thymine bands. In the interpretation of any change in secondary structure of KorB-N, possible contributions of DNA to the amide I and amide III regions must be taken into account.

In the 1200−1340 cm^{-1} region, troughs around 1207, 1252, 1298, 1317, and 1337 cm^{-1} are present; difference peaks are at 1215, 1237, and 1282 cm^{-1}. The trough at 1207 cm^{-1} can be assigned to Tyr and was discussed above.

The 1252 cm^{-1} trough is possibly caused by the diminished intensity of the amide III band at 1249 cm^{-1}, pointing to a reduction of unordered structures. Alternatively, changes in the 1256 cm^{-1} cytosine/thymine band must be considered the cause of the 1252 cm^{-1} trough. The large difference trough at 1668 cm^{-1} provides a further hint of the conformational changes reducing turns and irregular structures in the secondary structure of KorB-N.

Another difference feature in the amide III region is composed of a 1298 cm^{-1} trough and 1282 cm^{-1} peak. Amide III bands at 1273 and 1302 cm^{-1} are assigned to α-helices. The observed difference feature may be caused by intensity and/or frequency shifts of the helix vibrations, reflecting conformational changes in the protein, including helical structures. Of course, contributions from DNA might play a part in the formation of the difference feature.

Changes in α-helical structures are also suggested by the difference peaks at 937 and 1647 cm^{-1}. These difference peaks are at the 935 cm^{-1} band position assigned to the skeletal mode of α-helices and in the amide I region close to the 1653 cm^{-1} α-helix position, respectively.

Changes in Raman marker bands assigned to amino acid side chains, amide III bands, and amide I bands indicate restructuring of turns and unordered structures of KorB-N in the complex and imply DNA-dependent reorganization of the KorB-N structure. The observed spectral changes seem to indicate mainly changes in unordered and α-helix structures.

ACKNOWLEDGMENT

E.L. acknowledges the generous support of Hans Lehrach.

REFERENCES

1. Pansegrau, W., Lanka, E., Barth, P. T., Figurski, D. H., Guiney, D. G., Haas, D., Helinski, D. R., Schwab, H., Stanisich, V. A., and Thomas, C. M. (1994) Complete nucleotide sequence of Birmingham IncP plasmids: compilation and comparative analysis, *J. Mol. Biol. 239*, 623−663.
2. Delbrück, H., Ziegelin, G., Lanka, E., and Heinemann, U. (2002) An Src homology 3-like domain is responsible for dimerization of the repressor protein KorB encoded by the promiscuous IncP plasmid RP4, *J. Biol. Chem. 277*, 4191−4198.
3. Jagura-Burdzy, G., and Thomas, C. M. (1994) KorA protein of promiscuous plasmid RK2 controls a transcriptional switch between divergent operons for plasmid replication and conjugative transfer, *Proc. Natl. Acad. Sci. U.S.A. 91*, 10571−10575.
4. Jagura-Burdzy, G., and Thomas, C. M. (1997) Dissection of the switch between genes for replication and transfer of promiscuous plasmid RK2: basis of the dominance of *trfAp* over *trbAp* and specificity for KorA in controlling the switch, *J. Mol. Biol. 265*, 507−518.
5. Motallebi-Veshareh, M., Balzer, D., Lanka, E., Jagura-Burdzy, G., and Thomas, C. M. (1992) Conjugative transfer functions of broad-host-range plasmid RK2 are co-regulated with vegetative replication, *Mol. Microbiol. 6*, 907−920.
6. Zatyka, M., Jagura-Burdzy, G., and Thomas, C. M. (1994) Regulation of transfer genes of promiscuous IncP alpha plasmid RK2: repression of Tra1 region transcription both by relaxosome proteins and by the Tra2 regulator TrbA, *Microbiology 140*, 2981−2990.
7. Zatyka, M., Jagura-Burdzy, G., and Thomas, C. M. (1997) Transcriptional and translational control of the genes for the mating pair formation apparatus of promiscuous IncP plasmids, *J. Bacteriol. 179*, 7201−7209.
8. Łobocka, M., and Yarmolinsky, M. (1996) P1 plasmid partition: a mutational analysis of ParB, *J. Mol. Biol. 259*, 366−382.
9. Motallebi-Veshareh, M., Rouch, D., and Thomas, C. M. (1990) A family of ATPases involved in active partitioning of diverse bacterial plasmids, *Mol. Microbiol. 4*, 1455−1463.
10. Williams, D. R., and Thomas, C. M. (1992) Active partitioning of bacterial plasmids, *J. Gen. Microbiol. 138*, 1−16.
11. Williams, D. R., Macartney, D. P., and Thomas, C. M. (1998) The partitioning activity of the RK2 central control region requires only *incC*, *korB* and KorB-binding site O_B3 but other KorB-binding sites form destabilizing complexes in the absence of O_B3, *Microbiology 144*, 3369−3378.
12. Balzer, D., Ziegelin, G., Pansegrau, W., Kruft, V., and Lanka, E. (1992) KorB protein of promiscuous plasmid RP4 recognizes inverted sequence repetitions in regions essential for conjugative plasmid transfer, *Nucleic Acids Res. 20*, 1851−1858.
13. Jagura-Burdzy, G., Macartney, D. P., Zatyka, M., Cunliffe, L., Cooke, D., Huggins, C., Westblade, L., Khanim, F., and Thomas, C. M. (1999) Repression at a distance by the global regulator KorB of promiscuous IncP plasmids, *Mol. Microbiol. 32*, 519−532.
14. Macartney, D. P., Williams, D. R., Stafford, T., and Thomas, C. M. (1997) Divergence and conservation of the partitioning and global regulation functions in the central control region of the IncP plasmids RK2 and R751, *Microbiology 143*, 2167−2177.
15. Thomson, V. J., Jovanovic, O. S., Pohlman, R. F., Chang, C. H., and Figurski, D. H. (1993) Structure, function, and regulation of the *kilB* locus of promiscuous plasmid RK2, *J. Bacteriol. 175*, 2423−2435.
16. Benevides, J. M., Weiss, M. A., and Thomas, G. J., Jr. (1991) DNA recognition by the helix-turn-helix motif: investigation by laser Raman spectroscopy of the phage λ repressor and its interaction with operator sites O_L1 and O_R3, *Biochemistry 30*, 5955−5963.
17. Thomas, G. J., Jr., and Tsuboi, M. (1993) Raman spectroscopy of nucleic acids and their complexes, *Adv. Biophys. Chem. 3*, 1−70.
18. Thomas, G. J., Jr., and Wang, A. H.-J. (1988) Laser Raman spectroscopy of nucleic acids, *Nucleic Acids Mol. Biol. 2*, 1−30.

19. Benevides, J. M., Li, T., Lu, X.-J., Srinivasan, A. R., Olson, W. K., Weiss, M. A., and Thomas, G. J., Jr. (2000) Protein DNA directed structure II. Raman spectroscopy of a leucine zipper bZIP complex, *Biochemistry 39*, 548−556.
20. Krafft, C., Hinrichs, W., Orth, P., Saenger, W., and Welfle, H. (1998) Interaction of Tet repressor with operator DNA and with tetracycline studied by infrared and Raman spectroscopy, *Biophys. J. 74*, 63−71.
21. Overman, S. A., and Thomas, G. J., Jr. (1999) Raman markers of nonaromatic side chains in an α-helix assembly: Ala, Asp, Glu, Gly, Ile, Leu, Lys, Ser, and Val residues of phage fd subunits, *Biochemistry 38*, 4018−4027.
22. Peticolas, W. L. (1995) Raman spectroscopy of DNA and proteins, *Methods Enzymol. 246*, 389−416.
23. Siamwiza, M. N., Lord, R. C., Chen, M. C., Takamatsu, T., Harada, I., Matsuura, H., and Shimanouchi, T. (1975) Interpretation of the doublet at 850 and 830 cm^{-1} in the Raman spectra of tyrosyl residues in proteins and certain model compounds, *Biochemistry 14*, 4870−4876.
24. Miura, T., Takeuchi, H., and Harada, I. (1988) Characterization of individual tryptophan side chains in proteins using Raman spectroscopy and hydrogen deuterium exchange kinetics, *Biochemistry 27*, 88−94.
25. Miura, T., Takeuchi, H., and Harada, I. (1989) Tryptophan Raman bands sensitive to hydrogen bonding and side-chain conformation, *J. Raman Spectrosc. 20*, 667−671.
26. Benevides, J. M., Chan, G., Lu, X.-J., Olson, W. K., Weiss, M. A., and Thomas, G. J., Jr. (2000) Protein-directed DNA structure. I. Raman spectroscopy of a high-mobility-group box with application to human sex reversal, *Biochemistry 39*, 537−547.
27. Benevides, J. M., Kukolj, G., Autexier, C., Aubrey, K. L., DuBow, M. S., and Thomas, G. J., Jr. (1994) Secondary structure and interaction of phage D108 Ner repressor with a 61-base-pair operator: evidence for altered protein and DNA structures in the complex, *Biochemistry 33*, 10701−10710.
28. Benevides, J. M., Weiss, M. A., and Thomas, G. J., Jr. (1991) Design of the helix-turn-helix motif: nonlocal effects of quaternary structure in DNA recognition investigated by laser Raman spectroscopy, *Biochemistry 30*, 4381−4388.
29. Benevides, J. M., Weiss, M. A., and Thomas, G. J., Jr. (1994) An altered specificity mutation in the λ repressor induces global reorganization of the protein-DNA interface, *J. Biol. Chem. 269*, 10869−10878.
30. Deng, H., Bloomfield, V. A., Benevides, J. M., and Thomas, G. J., Jr. (1999) Dependence of the Raman signature of genomic B-DNA on nucleotide base sequence, *Biopolymers 50*, 656−666.
31. Dostál, L., Misselwitz, R., Laettig, S., Alonso, J. C., and Welfle, H. (2003) Raman spectroscopy of regulatory protein Omega from *Streptococcus pyogenes* plasmid pSM 19035 and complexes with operator DNA, *Spectroscopy 17*, 435−445.
32. Movileanu, L., Benevides, J. M., and Thomas, G. J., Jr. (1999) Temperature dependence of the Raman spectrum of DNA. Part I: Raman signatures of premelting and melting transitions of poly(dA-dT)·poly(dA-dT), *J. Raman Spectrosc. 30*, 637−649.

BI034723H